*Institute of Space and Aeronautical Science, University of Tokyo*
*Report No. 470, October 1971*

# Rotational Transitions in Para-Hydrogen by Molecular Collisions

*By*

Hisako SHIMAMURA and Kazuo TAKAYANAGI

*Summary*: The rotational transitions in molecular collisions in the para-hydrogen gas are theoretically studied in the distorted-wave approximation. In the long-range part of the intermolecular force, the orientation-dependence of the dipole-dipole dispersion force and the quadrupole-quadrupole interaction are fully taken into account. In the short-range part of the interaction, the anisotropy parameter is determined empirically in such a way as the calculated rate constants explain the ultrasonic absorption data at 90°K. It is shown that our rotational cross sections can explain satisfactorily the ultrasonic absorption experiment at 90° and 293°K, but the agreement with the ultrasonic dispersion experiment is less satisfactory. The orientation-dependence of the long-range interactions and the simultaneous transitions in two colliding molecules are both found important. Furthermore, it is found that the cross sections are large when the collision partner is in an excited state of rotation.

## 1. INTRODUCTION

Rotational transitions in molecular collisions in the hydrogen gas have been studied theoretically in several articles in the past. Early investigations (reviewed by Takayanagi [*1*][*2*]) are based on the simple exponentially repulsive interaction potential. As a more realistic interaction, Takayanagi [*3*] introduced the Morse type interaction and applied the modified wave number approximation [*4*] to calculate the cross section for the rotational excitation from the ground state $l=0$ to $l=2$, $l$ being the rotational quantum number. The potential function used was (see Fig. 1)

$$\begin{aligned} V(\boldsymbol{R}, \hat{\boldsymbol{r}}_1, \hat{\boldsymbol{r}}_2) = & D \exp\left[-2\alpha(R-R_0)\right] - 2D \exp\left[-\alpha(R-R_0)\right] \\ & + \beta D \exp\left[-2\alpha(R-R_0)\right]\left[P_2(\cos\chi_1)+P_2(\cos\chi_2)\right], \end{aligned} \tag{1}$$

where $\hat{\boldsymbol{r}}_i$ is the unit vector along the axis of the $i$th molecule, $\cos\chi_i = \hat{\boldsymbol{r}}_i \cdot \boldsymbol{R}$, and, in atomic units*,

$$D = 1.1 \times 10^{-4}$$
$$R_0 = 6.4$$

* We use atomic units throughout this paper, unless otherwise stated.

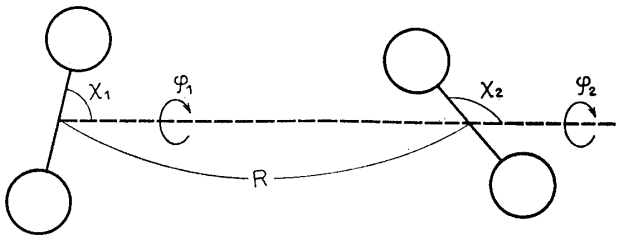


FIG. 1. Coordinates describing collision of two hydrogen molecules

$$\beta=0.075$$
$$2\alpha=1.87.$$

The parameters were chosen so as to obtain a good fit to the theoretical calculation of the short-range interaction by Evett and Margenau [5]. Later, Takayanagi [6] extended the calculation to excitations from excited states ($l=2\rightarrow l=4$, etc.). The same intermolecular potential was used by Davison [7] and by Roberts [8] in their full distorted-wave calculations. They found that a stronger angular dependence ($\beta\cong 0.14$) gave a closer agreement with experiments. Davison also used the following "exp-six" potential:

$$\begin{aligned} V(R,\chi_1,\chi_2)&=D\exp\left[-2\alpha(R-R_0)\right]-AR^{-6}\\ &+\{\beta D\exp\left[-2\alpha(R-R_0)\right]-BR^{-6}\}[P_2(\cos\chi_1)+P_2(\cos\chi_2)], \end{aligned} \tag{2}$$

where $D, \alpha$ and $R_0$ have the same values as before, and $A=11.0, B=0.8$ and $\beta$ is regarded as a parameter to be varied. The long-range $R^{-6}$ terms were based on the calculations of Britton and Bean [8].

Davison [9] proceeded to extend the distorted-wave calculations to the second order and found that the second-order correction lead to a decrease in the excitation cross section by several per cent at the thermal energy. Later, Allison and Dalgarno [10] studied the excitation $l=0\rightarrow l=2$ by a close-coupling method and found a cross section which was 15–20% smaller than the corresponding distorted-wave result in the energy range of 0.1–0.2 eV. These results are consistent with a more recent theoretical study by Roberts and Ross [11], who investigated the rotational transitions in $H_2$+He collisions with the second-order distorted-wave approximation, and found that the exact cross section is 20–30% smaller than the distorted wave result.

In the collision between two hydrogen molecules, the proper symmetrization of the wave function of the whole system is required. Such symmetrization for a pair of identical molecules has been discussed by Takayanagi [2][13], Gioumousis and Curtiss [14], Davison [7], and by Biolsi and Curtiss [15].

In almost all these works, one of the colliding molecules are assumed to remain in the ground state ($l=0$) throughout the collision, so that the collision problem is mathematically equivalent to the atom-diatom collision. It is one of the purposes of the present work to study the dependence of the rotational cross section on the rotational state of the collision partner. Very recently, Crawford [16] has studied

this problem qualitatively. He argues that the rotational cross sections increase when the collision partner is in a rotating state.

The simultaneous transitions

$$H_2(l=0)+H_2(l=4)\rightleftarrows H_2(l=2)+H_2(l=2) \tag{3}$$

were studied earlier by Takayanagi and Kishimoto [*17*], who found that these processes could not be neglected in studying the rotational relaxation in the hydrogen gas. The second purpose of the present article is to calculate the cross section for the processes (3) more accurately.

Finally, we tried to estimate the relative importance of the short-range and the long-range interactions in the rotational transitions.

## 2. Intermolecular Potential

The potential function adopted in the present work consists of four parts:

$$V(R,\chi_1,\chi_2,\varphi)=V_s+V_{dd}+V_{qq}+V_{dq}, \tag{4}$$

where $\varphi=\varphi_1-\varphi_2$. The first term $V_s$ represents the short-range repulsive interaction. The Evett-Margenau's potential [*5*], which we have used in previous calculations, is based on a rather simple form of the electronic wave function, so that it is not certain whether their $V_s$ is sufficiently accurate for our purpose. More recent calculations by Magnasco, Musso, and McWeeny [*18*][*19*] are restricted to a so limited range of the molecular orientation that their results, too, are not adequate for the present investigation. Thus we decided to use the short-range part of the Morse interaction (1)

$$\begin{aligned} V_s=&D\exp\left[-2\alpha(R-R_0)\right] \\ &+\beta D\exp\left[-2\alpha(R-R_0)\right]\left[P_2(\cos\chi_1)+P_2(\cos\chi_2)\right] \end{aligned} \tag{5}$$

and determine the parameter $\beta$ empirically (see § 5). As before, we take $D=1.1\times10^{-4}$, $2\alpha=1.87$ and $R_0=6.4$.

The second and third terms in (4) are the long-range interactions calculated by Britton and Bean [*9*]. We adopt their result without modification.

$$\begin{aligned} V_{dd}+V_{qq}=&-\frac{10.228}{R^6}+\frac{0.18312}{R^5} \\ &+\left[-\frac{1.03814}{R^6}-\frac{0.9156}{R^5}\right]\left[\cos^2\chi_1+\cos^2\chi_2\right] \\ &+\left[-\frac{0.06546}{R^6}+\frac{0.36624}{R^5}\right]\sin^2\chi_1\sin^2\chi_2\cos^2\varphi \\ &+\left[\frac{0.06546}{R^6}-\frac{0.73248}{R^5}\right]\sin 2\chi_1\sin 2\chi_2\cos\varphi \\ &+\left[-\frac{0.26184}{R^6}+\frac{3.11304}{R^5}\right]\cos^2\chi_1\cos^2\chi_2. \end{aligned} \tag{6}$$

Finally, for the higher-order dispersion term $V_{dq}$, we adopt the one averaged over the molecular orientation

$$V_{dq}=-116/R^8, \tag{7}$$

as estimated by Evett and Margenau [5]. The expressions in (6) and (7) are applicable only for large intermolecular separations. For the intermediate region of $R$, the error may be corrected to some extent by adjusting the parameter $\beta$ empirically. In order to avoid the singularities of (6) and (7) at origin, we add a hard core ($V=\infty$) for $R$ within 2.5 atomic units. Thus the adopted potential function becomes

$$\begin{aligned} V=&1.1\times10^{-4}\exp\left[-1.87(R-6.4)\right]+\frac{0.40693}{R^5}-\frac{11.0076}{R^6}-\frac{116}{R^8}\\ &+\left\{1.1\times10^{-4}\beta\exp\left[-1.87(R-6.4)\right]-\frac{0.82301}{R^6}\right.\\ &\qquad\left.+\frac{0.81387}{R^5}\right\}\left[P_2(\cos\chi_1)+P_2(\cos\chi_2)\right]\\ &+\left[-\frac{0.04364}{R^6}+\frac{0.24414}{R^5}\right]P_2(\cos\chi)\\ &+\left[-\frac{0.2618}{R^6}+\frac{2.84856}{R^5}\right]P_2(\cos\chi_1)P_2(\cos\chi_2)\\ &+\left[\frac{0.39276}{R^6}-\frac{3.6624}{R^5}\right]P_1(\cos\chi_1)P_1(\cos\chi_2)P_1(\cos\chi)\\ &\qquad\qquad\text{for } R>2.5\\ =&\ \infty \qquad\qquad\text{for } R\leqq2.5, \end{aligned} \tag{8}$$

where $\cos\chi=\hat{r}_1\cdot\hat{r}_2$.

In order to see the relative importance of the long-range part of the orientation-dependent interaction in the rotational excitation, some cross sections are calculated with the following potential, which is derived from (8) by averaging the long-range terms over the molecular orientation.

$$\begin{aligned} \bar{V}=&1.1\times10^{-4}\exp\left[-1.87(R-6.4)\right]-\frac{10.964}{R^6}-\frac{116}{R^8}\\ &+1.1\times10^{-4}\beta\exp\left[-1.87(R-6.4)\right]\left[P_2(\cos\chi_1)+P_2(\cos\chi_2)\right]\\ &\qquad\qquad\text{for } R>2.5\\ =&\ \infty \qquad\qquad\text{for } R\leqq2.5. \end{aligned} \tag{9}$$

## 3. Calculation of the Excitation Cross Sections and the Reaction Rates

The mathematical formulation of the distorted-wave method for our problem has been well established [2][7], so that only the basic formulae will be shown in the

following. The distorted waves $g(l_1l_2(L)jJ\,|\,k,R)$ are obtained by solving the radial equation of the form

$$\left[\frac{d^2}{dR^2}+k^2-\frac{j(j+1)}{R^2}-2\mu\xi(l_1l_2)\{(l_1l_2(L)jJ\,|\,V\,|\,l_1l_2(L)jJ)\right.$$
$$\left.+(-1)^z(l_2l_1(L)jJ\,|\,V\,|\,l_1l_2(L)jJ)\}\right]g(l_1l_2(L)jJ\,|\,k,R)=0, \tag{10}$$

with the usual boundary conditions

$$g(l_1l_2(L)jJ\,|\,k,R=0)=0, \tag{11a}$$

$$g(l_1l_2(L)jJ\,|\,k,R)\xrightarrow{R\to\infty}k^{-1}\sin\left(kR-\tfrac{1}{2}j\pi+\eta_n(k)\right), \tag{11b}$$

where $z=l_1+l_2-L+j$, $n=(l_1l_2(L)jJ)$, and

$$\xi(l_1l_2)=1/2 \qquad \text{for } l_1=l_2$$
$$=1 \qquad \text{for } l_1\neq l_2.$$

Because of the hard core in our potential (8), the condition (11a) is replaced in the present calculations by

$$g(l_1l_2(L)jJ\,|\,k,R=2.5)=0. \tag{11c}$$

The symbols $l_1$ and $l_2$ are the rotational quantum numbers of the colliding molecules before collision, and $L$ indicates the magnitude of the resultant rotational angular momentum ($L=|l_1-l_2|,\cdots,l_1+l_2$). The other symbols $j$ and $J$ represent the angular momentum of the orbital motion and the total angular momentum of the whole system, respectively ($j=|J-L|,\cdots,J+L$). When $l_1=l_2$, only the combinations $L-J=even$ are allowed. The distorted waves for the relative motion after the transition are similarly calculated with appropriate change of $l_1$, $l_2$, $L$, $j$, $J$ and $k$.

The effective cross section for the collisional transition

$$H_2(l_1)+H_2(l_2)\longrightarrow H_2(l_1')+H_2(l_2') \tag{12}$$

is then obtained by the formula

$$\sigma(l_1l_2\to l_1'l_2')=\frac{4\pi}{(2l_1+1)(2l_2+1)}\frac{k'}{k}\sum_J\sum_L\sum_{L'}\sum_j\sum_{j'}(2J+1)$$
$$\times\left|2\mu\int_0^\infty g(l_1'l_2'(L')j'J\,|\,k',R)\{(l_1'l_2'(L')j'J\,|\,V\,|\,l_1l_2(L)jJ)\right. \tag{13}$$
$$\left.+(-1)^{z'}(l_2'l_1'(L')j'J\,|\,V\,|\,l_1l_2(L)jJ)\}g(l_1l_2(L)jJ\,|\,k,R)dR\right|^2,$$

where $k$ and $k'$ are the wave numbers for the relative motion before and after the transition and $\mu$ is the reduced mass of the colliding system. The conservation of the energy of the system requires

$$\frac{k^2}{2\mu}+E_{l_1}+E_{l_2}=\frac{k'^2}{2\mu}+E_{l_1'}+E_{l_2'}, \tag{14}$$

where $E_l$ is the rotational energy of the molecule in the $l$th state.

The matrix elements of the intermolecular potential $V$ are defined by

$$\begin{aligned}&(l_1'l_2'(L')j'J\,|\,V\,|\,l_1l_2(L)jJ)\\&\quad=\int\mathscr{Y}_{JM}(l_1'l_2'(L')j'\,|\,\hat{\boldsymbol{R}},\hat{\boldsymbol{r}}_1,\hat{\boldsymbol{r}}_2)V(\boldsymbol{R},\hat{\boldsymbol{r}}_1,\hat{\boldsymbol{r}}_2)\mathscr{Y}_{JM}(l_1l_2(L)j\,|\,\hat{\boldsymbol{R}},\hat{\boldsymbol{r}}_1,\hat{\boldsymbol{r}}_2)d\hat{\boldsymbol{R}}d\hat{\boldsymbol{r}}_1d\hat{\boldsymbol{r}}_2,\end{aligned} \tag{15}$$

where

$$\begin{aligned}&\mathscr{Y}_{JM}(l_1l_2(L)j\,|\,\hat{\boldsymbol{R}},\hat{\boldsymbol{r}}_1,\hat{\boldsymbol{r}}_2)\\&\quad=\sum_{m_1}\sum_{m_2}(l_1l_2m_1m_2\,|\,l_1l_2L\;m_1+m_2)(Lj\;m_1+m_2\;M-m_1-m_2\,|\,LjJM)\\&\qquad\times Y(j\;M-m_1-m_2\,|\,\hat{\boldsymbol{R}})Y(l_1m_1\,|\,\hat{\boldsymbol{r}}_1)Y(l_2m_2\,|\,\hat{\boldsymbol{r}}_2).\end{aligned} \tag{16}$$

The quantities $(l_1l_2m_1m_2\,|\,l_1l_2L\;m_1+m_2)$, etc. are the Clebsch-Gordan coefficients and $Y$'s are the normalized spherical harmonics. It is noted that the integral (15) does not depend upon $M$. These matrix elements can be calculated by a method described in the Davison's paper [7].

It is important to notice that the above formulae are applicable to para-para collisions only. For para-ortho and ortho-ortho collisions, slight modifications are necessary [2].

The rate coefficient $K(l_1l_2\rightarrow l_1'l_2')$ is derived from the cross section (13) by averaging over the Maxwellian velocity distribution of molecules.

$$\begin{aligned}K(l_1l_2\rightarrow l_1'l_2')=\xi(l_1l_2)\xi(l_1'l_2')&\left(\frac{\mu}{2\pi\kappa T}\right)^{3/2}\\&\times\int_0^\infty\exp(-\mu v^2/2\kappa T)4\pi\sigma(l_1l_2\rightarrow l_1'l_2')v^3dv,\end{aligned} \tag{17}$$

where $\kappa$ is the Boltzmann constant, $v$ the relative velocity before collision $(=k/\mu)$, and $T$ the absolute temperature of the gas. The number of the process (12) taking place in unit time interval in unit volume of gas is given by

$$N(l_1)N(l_2)K(l_1l_2\rightarrow l_1'l_2'), \tag{18}$$

where $N(l)$ is the number density of hydrogen molecules in the $l$th rotational state. The factors $\xi(l_1l_2)\xi(l_1'l_2')$ are introduced in (17) to take account of the indistinguishability of the colliding molecules when they are in an identical state.

## 4. Ultrasonic Dispersion and Absorption

The experimental informations on the rotational transition probabilities under consideration come from the ultrasonic dispersion and absorption. The (complex) velocity $V$ of sound in a gas is given by [20]

$$V^2=\frac{RT}{M}\left\{1+2pB\frac{T_0^2}{T^2}+\frac{R}{C}\left(1+2p\frac{T_0^2}{T}\frac{dB}{dT}\right)\right\}, \tag{19}$$

where $R$ is the gas constant, $M$ the molecular weight, $T$ the temperature, $p$ the pressure, $B$ the second virial coefficient of the gas and $T_0=273°\mathrm{K}$. The heat capacity $C$ per mole at constant volume is a function of the temperature and the frequency of the sound $f$. The real part of $V$ gives the propagation velocity of the sound wave and the coefficient of absorption $\alpha$ due to rotational transitions is given by

$$\alpha/f=-2\pi ImV. \tag{20}$$

*Im* stands for the imaginary part. The experimental absorption coefficient corresponds to the sum of this rotational contribution and the classical absorption coefficient.

In this paper, we consider the pure para-hydrogen gas. The following transitions are taken into account.

$$H_2(0)+H_2(0)\underset{k_1}{\overset{k_1'}{\rightleftarrows}}H_2(2)+H_2(0) \tag{21}$$

$$H_2(0)+H_2(2)\underset{k_2}{\overset{k_2'}{\rightleftarrows}}H_2(2)+H_2(2) \tag{22}$$

$$H_2(2)+H_2(2)\underset{k_3}{\overset{k_3'}{\rightleftarrows}}H_2(0)+H_2(4) \tag{23}$$

$$H_2(2)+H_2(0)\underset{k_4}{\overset{k_4'}{\rightleftarrows}}H_2(4)+H_2(0) \tag{24}$$

$$H_2(2)+H_2(2)\underset{k_5}{\overset{k_5'}{\rightleftarrows}}H_2(4)+H_2(2). \tag{25}$$

If the number of molecules in the $l$th rotational state is $n_l$ per mole, we have $n_0+n_2+n_4\cong 6.02\times 10^{23}$, molecules in the 6th and higher rotational levels being neglected. Then the rate equations are

$$\frac{dn_4}{dt}=-k_3n_0n_4-k_4n_0n_4-k_5n_4n_2+k_3'n_2^2+k_4'n_2n_0+k_5'n_2^2, \tag{26}$$

$$\frac{dn_2}{dt}=-\frac{dn_0}{dt}-\frac{dn_4}{dt}, \tag{27}$$

$$\frac{dn_0}{dt}=-k_1'n_0^2-k_2'n_0n_2-k_3n_0n_4+k_1n_0n_2+k_2n_2^2+k_3'n_2^2, \tag{28}$$

where the rate constants $k$'s are easily obtained from $K$'s as

$$\begin{aligned} k_1'&=K(0,0\to 2,0)\frac{pT_0}{V_0p_0T},\\ k_1&=K(2,0\to 0,0)\frac{pT_0}{V_0p_0T}, \end{aligned} \tag{29}$$

$$k_2'=K(0,2\to 2,2)\frac{pT_0}{V_0p_0T},\quad \text{etc.},$$

where $p_0=1$ atm, $V_0=2.24\times 10^4$ cm$^3$/mol. From the principle of detailed balancing, we have

$$\frac{k_1'}{k_1}=\frac{k_2'}{k_2}=5\exp\left[-(E_2-E_0)/\kappa T\right]\equiv f_1(T), \tag{30}$$

$$\frac{k_4'}{k_4}=\frac{k_5'}{k_5}=\frac{9}{5}\exp\left[-(E_4-E_2)/\kappa T\right]\equiv f_2(T), \tag{31}$$

$$\frac{k_3'}{k_3}=\frac{9}{25}\exp\left[-(E_4-2E_2+E_0)/\kappa T\right]\equiv f_3(T), \tag{32}$$

$$E_l=2.69\times 10^{-4}l(l+1). \tag{33}$$

When a sound wave with a small amplitude propagates in the hydrogen gas, we have

$$T=T^0+\Delta Te^{i\omega t} \tag{34}$$

$$n_l=n_l^0+\Delta n_le^{i\omega t},\qquad \omega=2\pi f. \tag{35}$$

Substituting (30)–(35) into (26)–(28) and neglecting all the terms higher than the first-order ones with respect to $\Delta T$ and $\Delta n_l$, we obtain

$$\begin{aligned} i\omega\Delta n_4=&-k_3\left(n_0\Delta n_4+n_4\Delta n_0-2n_2\Delta n_2f_3-n_2^2\Delta T\frac{df_3}{dT}\right)\\ &-(k_4n_0+k_5n_2)\left(\Delta n_4-\Delta n_2f_2-n_2\Delta T\frac{df_2}{dT}\right), \end{aligned} \tag{36}$$

$$i\omega\Delta n_2=-\Delta n_0-\Delta n_4 \tag{37}$$

$$\begin{aligned} i\omega\Delta n_0=&-k_3\left(n_0\Delta n_4+n_4\Delta n_0-2n_2\Delta n_2f_3-n_2^2\Delta T\frac{df_3}{dT}\right)\\ &+(k_1n_0+k_2n_2)\left(\Delta n_2-\Delta n_0f_1-n_0\Delta T\frac{df_1}{dT}\right). \end{aligned} \tag{38}$$

After solving these equations to obtain $\Delta n_2/\Delta T$, $\Delta n_4/\Delta T$, the rotational contribution to the heat capacity is given by

$$C'=\frac{E_4\Delta n_4+E_2\Delta n_2}{\Delta T}. \tag{39}$$

The total heat capacity $C$, appearing in (19), can be obtained by

$$C=\frac{3}{2}R+C', \tag{40}$$

where $R$ is the gas constant.

## 5. Numerical Calculations and Results

Our programme for the numerical calculation of cross sections consists of three parts: Main programme, subprogramme A and subprogramme B. The values of $k$, $l_1, l_2, l_1', l_2'$ and $l_2'$ are initially put into the computer. Then the main programe calculates $k'$ from (14). For each value of $J(=0, 1, 2, \ldots)$ a finite number of sets $(j, j', L, L')$ are allowed by the selection rules. The subprogramme B is then called up. This programme calculates the matrix elements $(l_1'l_2'(L')j'J|V|l_1l_2(L)jJ)$ and the result is stored in the computer memory. The subprogramme A is for the solution of (10) by the Runge-Kutta method. The radial functions $f$'s thus obtained are stored in the memory. These calculations are repeated at 300 points for the intermolecular separation $R$ from 2.5 to 17.5. Then the product of the matrix element and $g$'s is integrated over $R$ by the Simpson method. Finally, the cross section (13) is obtained by taking sum over $J$, $L$, $L'$, $j$ and $j'$. The summation over $J$ is truncated at $J_1$ when the contribution for this value of $J$ is found to be less than $10^{-5}$ times the sum up to $J=J_1-1$. In order to save the computation time, we skipped calculations for some values of $J$ and later estimated those omitted contributions by interpolation. As a check of the programme, a calculation has been made with the Davison's "exp-six" potential (2). Our results agree with his values within a few percent.

In order to determine the adjustable parameter $\beta$ in our potential (8), low-

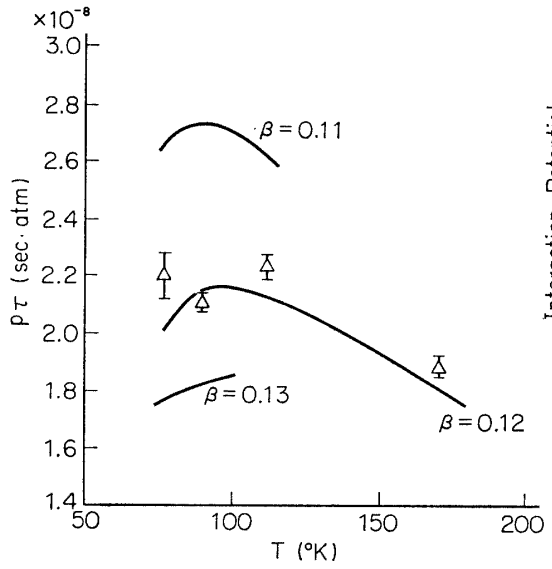


Fig. 2. Dependence of the rotational relaxation time on the anisotropy parameter $\beta$ at lower temperatures. The triangles with error bars are taken from Jonkman [22].

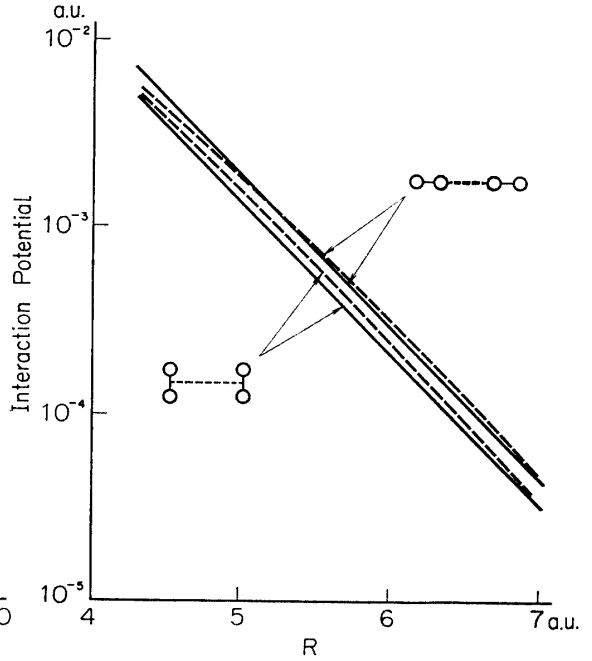


Fig. 3. Comparison of the short-range part of interaction adopted in the present work (solid curves) and the theoretical potential of Evett and Margenau [5] (dashed curves) for the two relative configurations of colliding molecules, as indicated in the figure.

temperature ultrasonic absorption data were used. At sufficiently low temperatures, our problem practically becomes a two-level problem and the reactions (22)–(25) can be neglected without introducing an important error. The relaxation time $\tau$ is thus obtained by

$$\frac{1}{\tau}=NK(0,0\rightarrow 0,2)+NK(0,2\rightarrow 0,0), \tag{41}$$

where $N$ is the number density of collision partners, most of which are in the $l=0$

TABLE 1. $\xi(l_1l_2)\xi(l_1'l_2')\sigma(l_1l_2\rightarrow l_1'l_2')$ in atomic units ($a_0^2=2.8\times10^{-17}\text{cm}^2$) calculated with the potential $V$ in eq. (8)

| $k$ a.u. | $E$ eV | (0,0→0,2) | (0,2→2,2) | (0,2→0,4) | (2,2→2,4) | (2,2→0,4) |
|---|---|---|---|---|---|---|
| 2.5 | 0.046 | 0.038 | 0.064 | | | |
| 3.0 | 0.067 | 0.288 | 0.516 | | | 0.0065 |
| 3.5 | 0.091 | 0.675 | 1.22 | | | 0.0443 |
| 4.0 | 0.118 | 1.15 | 2.02 | | | 0.107 |
| 4.1 | 0.124 | | | 0.0118 | | |
| 4.4 | 0.143 | | | 0.0349 | | |
| 4.5 | 0.150 | 1.70 | 2.81 | | 0.054 | 0.186 |
| 4.7 | 0.164 | | | 0.077 | | |
| 5.0 | 0.185 | 2.30 | 3.58 | 0.134 | 0.16 | 0.26 |
| 5.3 | 0.208 | | | 0.210 | | |
| 5.5 | 0.224 | 2.95 | | | 0.34 | |
| 5.6 | 0.232 | | | 0.308 | | |
| 5.9 | 0.258 | | | 0.424 | | |
| 6.0 | 0.267 | | | | 0.54 | |

($k$, wave nnmber; $E$, kinetic energy of relative motion before collision)

TABLE 2. $\xi(l_1l_2)\xi(l_1'l_2')\sigma(l_1l_2\rightarrow l_1'l_2')$ in atomic units ($a_0^2=2.80\times10^{-17}\text{cm}^2$) calculated with the potential $\tilde{V}$ in eq. (9)

| $k$ a.u. | $E$ eV | (0,0→0,2) | (0,2→2,2) | (0,2→0,4) | (2,2→2,4) |
|---|---|---|---|---|---|
| 2.5 | 0.046 | 0.0604 | | | |
| 3.0 | 0.067 | 0.447 | 0.448 | | |
| 3.5 | 0.091 | 1.04 | 1.06 | | |
| 4.0 | 0.118 | 1.77 | 1.78 | | |
| 4.1 | 0.124 | | | 0.015 | 0.015 |
| 4.5 | 0.150 | 2.59 | | | |
| 4.6 | 0.157 | | | 0.077 | 0.077 |
| 5.0 | 0.185 | 3.47 | 3.50 | | |
| 5.1 | 0.193 | | | 0.20 | 0.20 |
| 5.6 | 0.232 | | | 0.46 | |
| 6.1 | 0.276 | | | 0.85 | |

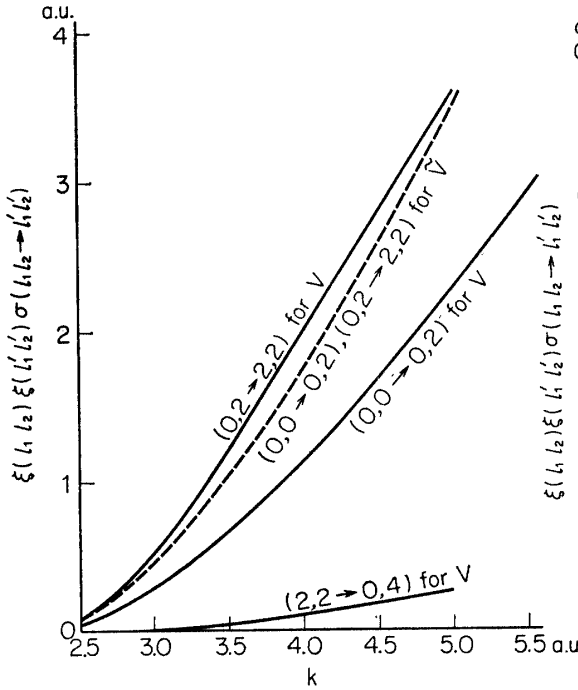


FIG. 4. Effective cross sections $\sigma(0,0\to0,2)$, $\sigma(0,2\to2,2)$ and $\sigma(2,2\to0,4)$. Solid curves are obtained with the potential (8) and dashed curves are obtained with the partially averaged potential (9). For the potential (9), the difference between $\sigma(0,0\to0,2)$ and $\sigma(0,2\to2,2)$ is too small to be shown in the figure.

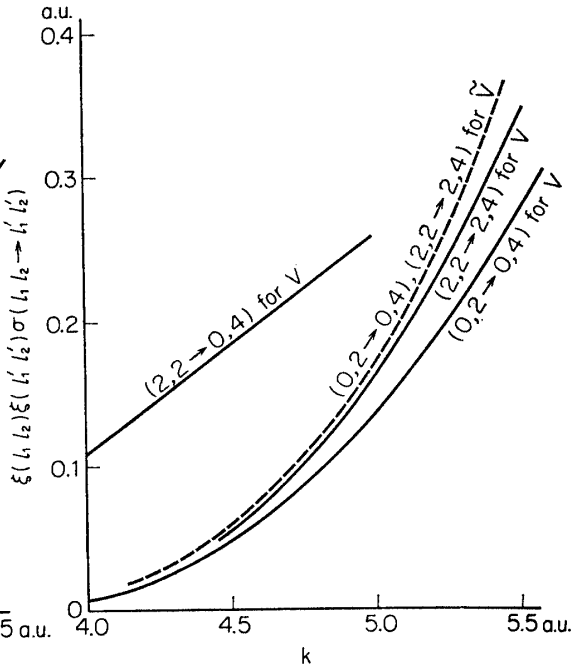


FIG. 5. Effective cross sections $\sigma(0,2\to0,4)$ and $\sigma(2,2\to2,4)$ for the potentials (8) and (9). For the potential (9), these two cross sections coincide within the accuracy of the present calculations.

state. The relaxation time $\tau$ is calculated for $\beta=0.11$, 0.12 and 0.13 and the results are compared with the experimental data [*21*][*22*] in Fig. 2. The high-temperature part of the curve for $\beta=0.12$ is not so accurate since the simple formula (41) becomes inappropriate as the temperature rises. As is seen in Fig. 2, the best value of $\beta$ is about 0.12. This is compared with the Davison's value $\beta=$ 0.14 which he has estimated with his potential (2). The short-range part of our potential thus determined is compared with the theoretical calculation by Evett and Margenau [*5*] for two relative orientations in Fig. 3.

The calculated cross sections are shown in Tables 1 and 2, and in Figs. 4 and 5. It is clearly seen from these tables and figures that the potential (8) and the potential (9) give considerably different cross sections. In other words, the direct contribution of the van der Waals interaction to the rotational transitions can not be neglected.

Another interesting feature of our result is that the excitation cross section becomes large when the collision partner is in an excited state of rotation. This is in agreement with the conclusion of a qualitative argument by Crawford [*16*]. According to the present calculation, however, this effect of the rotation of collision

partner practically disappears when the potential (9) is used, i.e., when the transitions are caused by the short-range interaction only.

The simultaneous transitions $(2, 2 \rightleftarrows 0, 4)$ are of the higher order from the viewpoint of the perturbation theory. Nevertheless, it is found that the cross sections for these processes are fairly large. In fact, the process $(2,2 \rightarrow 0,4)$ is the most important process for the production of the $l=4$ state in the intermediate energy region, provided that the number density N(2) of molecules in the $l=2$ state is not too low.

## 6. Comparison with Experiments. Discussions.

The rate coefficients $K(l_1 l_2 \rightarrow l_1' l_2')$ are calculated from our cross sections by the integration (17). The results are presented in Table 3. The ultrasonic absorption and dispersion curves are now obtained as was described in §4.

At 90°K, where we empirically determined $\beta$, the only adjustable parameter in our work, the rotational absorption curve from the theoretical calculation agrees very satisfactorily with experimental values [*21*] as is seen in Fig. 6.

Table 3. Rate coefficients $K(l_1 l_2 \rightarrow l_1' l_2')$ in $cm^3/sec$

| process \ temperature | 90°K | 197.1°K | 293°K | 298.4°K |
|---|---|---|---|---|
| $(0,0 \rightarrow 0,2)$ | 9.6(−15)* | 4.7(−13) | 1.7(−12) | 1.8(−12) |
| $(0,2 \rightarrow 2,2)$ | 7.5(−15) | 8.0(−13) | 2.8(−12) | 2.9(−12) |
| $(0,2 \rightarrow 0,4)$ | | 1.6(−15) | 2.2(−14) | 2.4(−14) |
| $(2,2 \rightarrow 2,4)$ | | 1.7(−15) | 2.5(−14) | 2.8(−14) |
| $(2,2 \rightarrow 0,4)$ | | 2.4(−14) | 1.2(−13) | 1.3(−13) |

*) (−15), etc. stand for $\times 10^{-15}$, etc.

In Fig. 7, the calculated absorption due to the rotational relaxation at 293°K (solid line) is compared with experimental data of Sluijter [*21*]. The agreement is fairly good, but a slight difference is noticeable at lower frequency side of the absorption maximum. In this respect, we may consider that the two largest cross sections $\sigma(0, 0 \rightarrow 0, 2)$ and $\sigma(0, 2 \rightarrow 2, 2)$ have been overestimated in the present calculation, since the distorted-wave method is a perturbation method where all the transition probabilities are assumed small. Thus we arbitrarily replace the corresponding rate coefficients $K(0,0 \rightarrow 0,2)$ and $K(0,2 \rightarrow 2,2)$ by somewhat smaller values and obtained the dashed curve in Fig. 7. The agreement with experiment is now very good at lower frequencies, but the agreement at higher frequencies is lost.

Fig. 8 presents the ultrasonic dispersion curves at 298.4°K. The theoretical curve (solid line) is compared with experimental values by Rhodes [*23*] and by Geide [*24*]. There is a considerable discrepancy between theory and experiment. This discrepancy almost disappears (as in the dashed curve in Fig. 8) when we replace the two largest rate coefficients $K(0,0 \rightarrow 0,2)$ and $K(0,2 \rightarrow 2,2)$ by some-

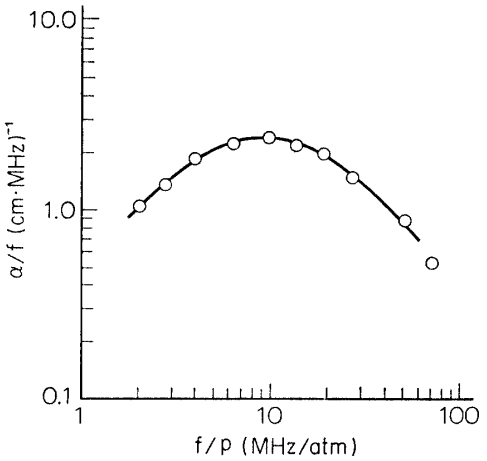


FIG. 6. Ultrasonic absorption due to rotational relaxation at 90°K. Solid curve is the theoretical result calculated from (19), (20), (40) and circles are experimental values of Sluijter [21].

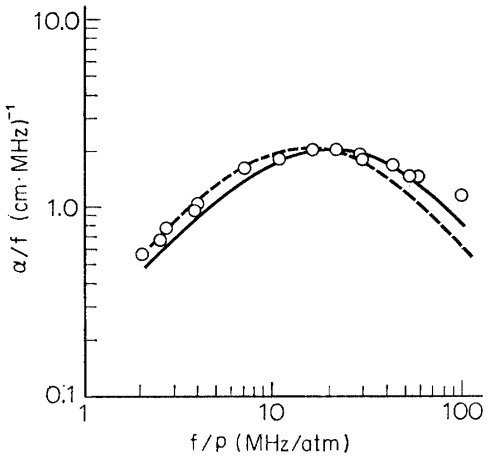


FIG. 7. Ultrasonic absorption due to rotational relaxation at 293°K. Solid curve is the result of theoretical calculation with the distorted-wave cross sections. Dashed curve is obtained by modifying values of the two largest rate coefficients as $K(0,0\rightarrow 0,2)=1.320\times 10^{-12}$ cm³/sec, $K(0,2\rightarrow 2,2)=2.015\times 10^{-12}$ cm³/sec.

what smaller values, just as we did in Fig. 7. However, we have already seen that such modifications lead to the disagreement of theory and experiment in the absorption curve at higher frequencies. Thus, there seems to be some inconsistency between ultrasonic dispersion and absorption data.

The distorted-wave method, generally, overestimates excitation cross sections. Even in the neighborhood of the threshold of the rotational excitation, there is an

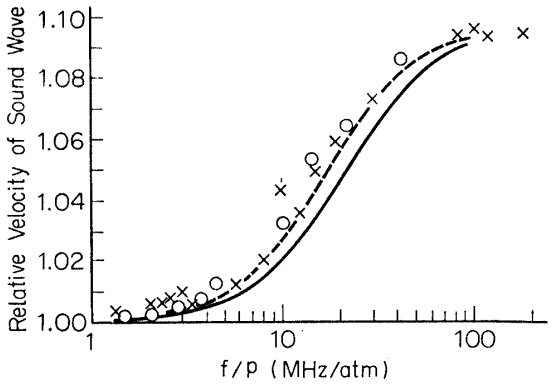


FIG. 8. Ultrasonic dispersion due to rotational relaxation at 298.4°K. The ratio of the sound velocity to its value at low-frequency limit ($f\rightarrow 0$) is plotted against $f/p$. The solid curve is obtained by using the distorted-wave cross sections. The dashed curve is obtained by using the rate coefficients $K(0,0\rightarrow 0,2)=1.402\times 10^{-12}$cm³/sec and $K(0,2\rightarrow 2,2)=2.104\times 10^{-12}$cm³/sec. Other rate coefficients remain unchanged. This set of modified rate coefficients is in much better agreement with experimental data (circles: Rhodes [23]; crosses: Geide [24]).

overestimation by 10–20% (see §1). This defect is partly avoided in the present work by choosing the anisotropy parameter $\beta$ empirically. However, as the collision energy increases, the excitation probability increases also. Then the deviation of the first-order perturbation theory from the correct situation becomes more serious. On the other hand, the defect of the distorted-wave method should be less serious at lower energies. From this point of view, it is hard to understand why the discrepancy between theory and dispersion experiment is still considerable at a temperature as low as 190°K (figures not shown in this paper).

As was pointed out in the introduction, most previous papers assumed that the collision partners were in the lowest state of rotation. Or, equivalently, it is tacitly assumed for simplicity that the rotational transition in a molecule does not depend much on the rotational state of the collision partner. To see the effect of the rotational state of collision partner, ultrasonic absorption curves are presented in Fig. 9.

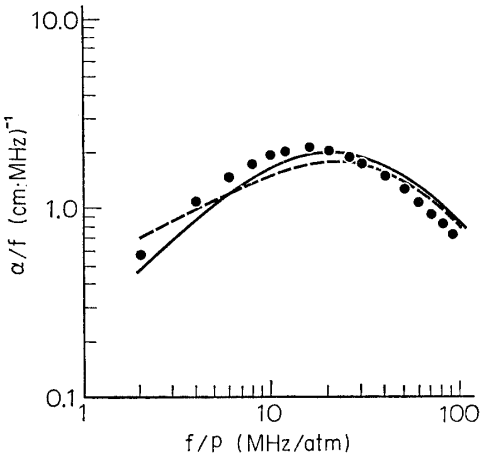


FIG. 9. Ultrasonic absorption due to rotational relaxation at 293°K. The solid curve is the same as in Fig. 7. The dashed curve is obtained by neglecting the processes (23), i.e., by putting $K(2,2\rightarrow 0,4)=0$. The dots are obtained by putting $K(0,2\rightarrow 2,2)=K(0,0\rightarrow 0,2)=1.7\times 10^{-12}\mathrm{cm}^3/\mathrm{sec}$, $K(2,2\rightarrow 2,4)=K(0,2\rightarrow 0,4)=2.2\times 10^{-14}\mathrm{cm}^3/\mathrm{sec}$, and $K(2,2\rightarrow 0,4)=1.2\times 10^{-13}\mathrm{cm}^3/\mathrm{sec}$.

The solid curve is based on the rate coefficients as in Table 3, while the dots were obtained by assuming that $K(0,2\rightarrow 2,2)$ is equal to $K(0,0\rightarrow 0,2)$, and that $K(2,2\rightarrow 2,4)$ is equal to $K(0,2\rightarrow 0,4)$. As is seen in the figure, the simplifying assumption leads to an appreciable error. Similarly, the dashed curve, which was obtained by entirely neglecting the simultaneous transitions (23), is quite different from the solid curve, especially at low-frequency region.

We conclude that, in studying the rotational transitions in molecular collisions, the quantitatively accurate intermolecular force must be used and all the relevant processes must be taken into account. Only this kind of full theoretical calculations can interpret experimental data properly and test the consistency of ultrasonic absorption and dispersion data. The single-relaxation-time treatment, for instance, is not appropriate for data analysis except at lowest temperatures. The accuracy

of the present work is still limited because of the lack of knowledge of sufficiently accurate intermolecular interaction, especially at short distances, and because of our use of the distorted-wave method.

The numerical computations in the present work have been carried out on the computer HITAC 5020F at the Data Processing Center, Institute of Space and Aeronautical Science.

*Department of Space Science*
*Institute of Space and Aeronautical Science*
*University of Tokyo*
*July, 1971*

## References

[1] K. Takayanagi: Progr. Theor. Phys. suppl. No. **25**, 1 (1963).
[2] K. Takayanagi: Adv. Atom. Mol. Phys. **1**, 149 (1965).
[3] K. Takayanagi: Proc. Phys. Soc. A**70**, 348 (1957).
[4] K. Takayanagi: Progr. Theor. Phys. 8, 497 (1952); see also references [1] [2].
[5] A. A. Evett and H. Margenau: Phys. Rev. **90**, 1021 (1953).
[6] K. Takayanagi: Sci. Rep. Saitama Univ. A**3**, No. 2, 87 (1959).
[7] W. D. Davison: Discussions Faraday Soc. **33**, 71 (1962).
[8] C. S. Roberts: Phys. Rev. **131**, 209 (1963).
[9] F. R. Britton and D. T. W. Bean: Can. J. Phys. **33**, 668 (1955).
[10] W. D. Davison: Proc. Roy. Soc. A**280**, 227 (1964).
[11] A. C. Allison and A. Dalgarno: Proc. Phys. Soc. **90**, 609 (1967).
[12] R. E. Roberts and J. Ross: J. Chem. Phys. **52**, 5011 (1970).
[13] K. Takayanagi: Progr. Theor. Phys. **11**, 557 (1954).
[14] G. Gioumousis and C. F. Curtiss: J. Chem. Phys. **29**, 996 (1958).
[15] L. Biolsi and C. F. Curtiss: J. Chem. Phys. 48, 4508 (1968).
[16] O. H. Crawford: Chem. Phys. Letters **6**, 409 (1970).
[17] K. Takayanagi and T. Kishimoto: Progr. Theor. Phys. **9**, 578 (1953); **10**, 369 (1953).
[18] V. Magnasco and G. F. Musso: J. Chem. Phys. **46**, 4015 (1967); **47**, 1723 (1967); **47**, 4629 (1967).
[19] V. Magnasco, G. F. Musso and R. McWeeny: J. Chem. Phys. **47**, 4617 (1967).
[20] see, e.g., K. F. Herzfeld and T. A. Litovitz: Absorption and Dispersion of Ultrasonic Waves, Academic Press (1959).
[21] C. G. Sluijter: Investigations of Translational-Rotational Relaxations in Hydrogen Isotopes (thesis, Leiden University) (1964).
[22] R. M. Jonkman: Rotational Relaxation in Hydrogen Isotope-Noble Gas Mixtures, thesis, Leiden University (1967).
[23] J. E. Rhodes: Phys. Rev. **70**, 932 (1946).
[24] K. Geide: Acustica **13**, 31 (1963).